2011

Effect of Grain Size on Uranium(VI) Surface Complexation Kinetics and Adsorption Additivity

Jianying Shang
Pacific Northwest National Laboratory

Chongxuan Liu
Pacific Northwest National Laboratory, chongxuan.liu@pnl.gov

Zheming Wang
Pacific Northwest National Laboratory, Zheming.wang@pnl.gov

John M. Zachara
Pacific Northwest National Laboratory, john.zachara@pnl.gov

Environmental Science & Technology

ARTICLE

pubs.acs.org/est

Effect of Grain Size on Uranium(VI) Surface Complexation Kinetics and Adsorption Additivity

Jianying Shang, Chongxuan Liu,* Zheming Wang, and John M. Zachara

Pacific Northwest National Laboratory, Richland, Washington 99354, United States

Supporting Information

ABSTRACT: The contribution of variable grain sizes to uranium adsorption/desorption was studied using a sediment from the US DOE Hanford site. The sediment was wet sieved into four size fractions: coarse sand (1−2 mm), medium sand (0.2−1 mm), fine sand (0.053−0.2 mm), and clay/silt fraction (<0.053 mm). For each size fraction and their composite (sediment), batch and flow-cell experiments were performed to determine uranium adsorption isotherms and kinetic uranium adsorption and subsequent desorption. The results showed that uranium adsorption isotherms and adsorption/desorption kinetics were size specific, reflecting the effects of size-specific adsorption site concentration and kinetic rate constants. The larger-size fraction had a larger mass percentage in the sediment but with a smaller adsorption site concentration and generally a slower uranium adsorption/desorption rate. The same equilibrium surface complexation reaction and reaction constant could describe uranium adsorption isotherms for all size fractions and the composite after accounting for the effect of adsorption site concentration. Mass-weighted, linear additivity was observed for both uranium adsorption isotherms and adsorption/desorption kinetics in the composite. One important implication of this study is that grain-size distribution may be used to estimate uranium adsorption site and adsorption/desorption kinetic rates in heterogeneous sediments from a common location.

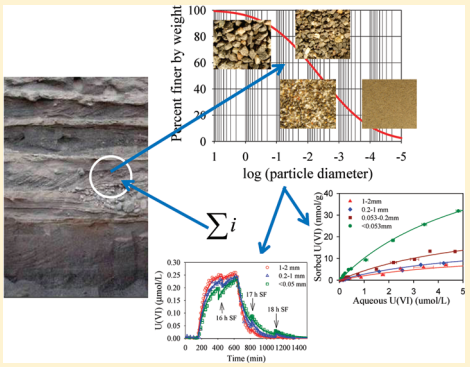

INTRODUCTION

Grain size is an important sediment property that affects solute and contaminant sorption and desorption.[1] A sediment typically consists of various sizes of grains ranging from clay to sand, gravel, or pebble. Uranium, however, primarily resides in grains of less than 2 mm size.[2−4] Extensive research has consequently been performed to investigate uranium adsorption/desorption reactions and kinetics in the <2 mm size fraction in sediments.[4−12] The reactions and kinetics determined from the <2 mm size fraction are then used to predict uranium adsorption/desorption behavior in field-textured sediments by assuming that the adsorption reactions, reaction constants, and kinetic parameters in the reactive (<2 mm) and nonreactive (>2 mm) size fractions can be linearly added up.[3,11,13−15] The linear additivity assumption with respect to size fractions, however, has not been rigorously evaluated.

Uranyl [U(VI)] adsorption/desorption reactions are typically described using surface complexation (SC) reactions either by considering additive contributions from individual minerals or by selecting a few "generic" reactions that best match experimental results.[2,16−19] The later approach is considered as an upscaled model for sediments containing complex mixtures of minerals.[20] Recent studies found that U(VI) adsorption/desorption reactions are kinetic processes that are apparently rate limited by intragranular diffusive mass transfer.[9,12,21] The grain-scale diffusion controls reactant supply and product removal for SC reactions in intragrain pore domains. One important parameter that affects the grain-scale diffusion is the grain size, which not only affects the apparent length of diffusion paths but also affects pore volume, connectivity, and their distribution in intragrain domains that fundamentally affect diffusion rate.[22]

In this study, we investigated the contribution of various grain sizes to U(VI) adsorption/desorption and kinetic behavior in a sediment. Batch and stirred flow-cell experiments were conducted to derive equilibrium and kinetic data, and numerical modeling was performed to interpret the experimental results and to derive reaction and kinetic parameters in individual size fractions. The experimental data and size-specific reactions and kinetic parameters were then used to determine the contribution of different grain sizes to the overall adsorption/desorption and kinetics in the sediment and to evaluate additivity concept with respect to grain size by comparing calculated and measured U(VI) adsorption and kinetics in the composite.

MATERIALS AND METHODS

Sediment Preparation. The sediment used in this study was collected from the Integrated Field Research Challenge (IFRC) site in the US Department of Energy (DOE) Hanford 300 Area.

Received: March 27, 2011
Accepted: June 7, 2011
Revised: June 3, 2011
Published: June 07, 2011

Table 1. Synthetic Groundwater (SGW) Chemical Composition (mmol/L)

Ca	Mg	Na	K	Cl	NO_3	SO_4	CO_2(tot)	pH
1.00	0.51	1.44	0.16	1.30	0.47	0.64	1.57	7.9

Contaminant uranium (96 μg/kg) in the sediment was partially removed by desorption in a column system using a synthetic IFRC groundwater (SGW) with its chemical composition provided in Table 1. The treated sediment was wet sieved into four size fractions: coarse sand (1−2 mm), medium sand (0.2−1 mm), fine sand (0.053−0.2 mm), and clay/silt (<0.053 mm). The four size fractions and their composite (i.e., <2 mm fraction in the sediment) were further treated to remove residual U by suspending them in the SGW solution (100 g/L) for 1 week (1−2, 0.2−1, and 0.053−0.2 mm and the composite) or 2 weeks (<0.053 mm). The U-removed samples were collected by centrifugation and used in experiments.

Sediment Characterization. The surface areas of each size fraction and their composite were measured by the Brunauer−Emmett−Teller (BET) method (Quantachrome Autosorb Automated Gas Sorption Systems). Micropore size distributions and pore volume were calculated by the BJH method[23,24] from N_2 adsorption and desorption isotherms.[25] The mineralogical composition in each grain-size fraction was determined by X-ray diffraction and the Powder Diffraction File database (ICDD PDF-2, 2010) for reference diffraction data from the International Center for Diffraction Data.

U Sorption Isotherms. For each size fraction and their composite, batch experiments were performed to determine U(VI) partitioning between aqueous and solid phases in the SGW solution (Table 1) as a function of aqueous U(VI) concentration. The solid/SGW solution suspensions (100 g/L) were spiked with U(VI) as $UO_2(NO_3)_2$ with a final U(VI) concentration from 10 to 2000 μg/L, equilibrated for 1 week on a reciprocal shaker, and then centrifuged for 30 min (3600 RFC) for phase separation. Independent experiments found that uranyl adsorption reached steady state after 1 week of equilibration. The supernatants in the centrifuged suspensions were collected by filtration (0.20 um) for chemical analysis after discarding the first a few droplets of the filtrates. Uranyl concentration in the filtrates was analyzed using a kinetic phosphorescence analyzer (KPA, Chemchek Instruments, Richland, WA). Cations Ca, K, Mg, Si, and Na were measured using an inductively coupled plasma-optical emission spectrometer (ICP-OES, Perkin-Elmer, Optima 2100DV), and total dissolved inorganic carbon was determined using a carbon analyzer (Dohrman carbon analyzer, DC-80). The adsorbed U was calculated from the difference between total added U(VI) and measured final aqueous U(VI) concentration in the suspension.

Kinetic Experiments. Grain-scale kinetics of U(VI) adsorption/desorption was determined in a stirred flow-cell reactor (2.2 cm ID, 3 cm length, and 11 mL total volume). The reactor was equipped with an influent port at the bottom and effluent port on the top. The SGW was injected into the reactor by a peristaltic pump (Cole-Parmer, IL), and effluent was collected using an automatic fraction collector (Teledyne, NE). Both ports were equipped with a porous frit with a pore size of 10 μm to generate a uniform flow, and the effluent port was equipped with a 0.2 μm pore size membrane to contain solids. The stirred-flow experiments were performed at a constant flow rate of 0.16 mL/min with a solid/solution ratio of 260 g/L.

U(VI)-containing solution was prepared by spiking the SGW with $UO_2(NO_3)_2$ with a final concentration of 60 ug/L U(VI). To evaluate the physical mixing in the reactor, the U(VI)-containing SGW was also spiked with NaBr with a final concentration of 5 mg/L Br. The U(VI)-free SGW solution was first introduced into the flow-cell reactor for at least 2.5 h to chemically equilibrate the solids with the SGW solution before injecting the U(VI)-containing solution. The solids in the flow-cell reactor were mixed with the SGW solution using a magnetic stir bar. The influent flow was periodically interrupted (i.e., flow-stop-flow mode) to probe the kinetic response of U(VI) adsorption/desorption to the residence time of mixing fluids. The effluents were collected every 10 min by a fraction collector for U(VI) and other chemical analyses as described previously.

Modeling. The following SC reaction, which was determined under variable chemical conditions for the IFRC sediments,[26] was used to describe U(VI) adsorption/desorption reaction

$$>\mathrm{SOH} + \mathrm{UO_2}^{2+} + 2\mathrm{CO_3}^{2-} = >\mathrm{SOUO_2(CO_3HCO_3)}^{2-} \quad (1)$$

where >SOH denotes the surface site and $>SOUO_2(CO_3HCO_3)^{2-}$ is the sorbed U(VI) species. The reaction equilibrium constant for each size fraction was estimated from the isotherms as described in the following section.

The kinetics of U(VI) adsorption/desorption was described using a multirate SC model that was previously developed to represent diffusion-limited U(VI) SC reactions[9]

$$\frac{\partial C_i}{\partial t} + \frac{(1-\theta)\rho_s}{\theta}\sum_{j=1}^{N_s} a_{ij}\sum_{k=1}^{M_j}\frac{\partial q_j^k}{\partial t} = L(C_i), i = 1, 2, ..., N_c \quad (2)$$

$$\frac{\partial q_j^k}{\partial t} = \alpha_j^k(Q_j^k - q_j^k), j = 1, 2, ..., N_s; k = 1, 2, ..., M \quad (3)$$

where C_i is the total aqueous concentration of chemical component i (mol/L), θ is the porosity, ρ_s is the solid density (kg/L), a_{ij} is the stoichiometric coefficient of chemical component i in adsorbed species j, N_c is the number of chemical components, q_j^k is the concentration of adsorbed species j at adsorption site k (mol/kg), α_j^k is the rate constant of adsorbed species j at adsorption site k (min^{-1}), Q_j^k is the concentration of adsorbed species j at adsorption site k (mol/kg) in equilibrium with bulk solution chemistry, N_s is the number of adsorbed species, and M is the number of adsorption sites. $L(C_i)$ is the transport term, which has the following form for the stirred flow-cell reactor

$$L(C_i) = F(C_i^{in} - C_i)/V \quad (4)$$

where F is the flow rate (mL/min), V is the aqueous volume of the flow-cell reactor (mL), and C_i^{in} is the total concentration of chemical component i in the influent solution. The equilibrium-adsorbed concentration Q_j^k in eq 3 is calculated from the mass action equation of the adsorption reaction (eq 1). The rate constant α_j^k in eq 3 was assumed to follow the log-normal probability distribution $p(\alpha)$ to minimize the number of parameters in the model

$$p(\alpha) = \frac{1}{\sqrt{2\pi}\alpha\sigma}exp\left(-\frac{1}{2\sigma^2}(ln(\alpha)-\mu)^2\right) \quad (5)$$

where μ and σ are the two parameters that define the probability distribution.

Table 2. Sediment Properties

	size fraction (mm)					
	<0.053	0.053 < size < 0.2	0.2 < size < 1	1 < size < 2	composite (<2 mm)	composite (<2 mm) predicted
mass fraction (%)	8.70 ± 1.37	6.50 ± 0.57	48.14 ± 0.79	36.67 ± 1.15	NA	NA
surface area (m^2/g)	13.53	7.28	7.96	8.14	10.80	8.5
pore volume (mm^3/g)	51.48	19.3	13.18	11.07	17.00	16.13

Ten chemical components were considered in the modeling including UO_2, Ca, Mg, Na, K, CO_2(tot), H, NO_3, SO_4, and <SOH. A total of 46 aqueous and surface species that were uniquely defined by the linear combination of the 10 chemical components were used in the model. These chemical components and species affected the ionic activities involved in the uranyl surface complexation reaction. The aqueous speciation reactions used in this study were described elsewhere,[9] and the surface complexation reaction was described by eq 1.

RESULTS AND DISCUSSION

Sediment Properties. The sediment consisted of 52% gravel and cobble (>2 mm) and 48% of the <2 mm size fraction. Only the <2 mm size solids were used in this study because of the exclusive U(VI) association with this size fraction.[3,27] The <2 mm size fraction consisted of 37%, 48%, 6.5%, and 8.7% of coarse sand, medium sand, fine sand, and silt/clay, respectively (Table 2). The minerals detected by the X-ray diffraction analysis were the same for all size fractions: quartz, feldspar (albite and anorthite), corundum, and pyroxene. Clinochore, muscovite, smectite, and vermiculite were identified in the silt/clay fraction after clay minerals were isolated through sedimentation. The clay minerals were, however, minor components and below detection when they were in the silt/clay size fraction.

The silt/clay size fraction had the largest BET surface area, as expected, after normalizing to its solid mass (Table 2). The surface area in the other three size fractions was only slightly different. The similar surface area in the coarse grain sizes in the Hanford sediments was observed previously.[28] The surface area in the composite calculated from the mass-weighted, linear addition of the surface areas in individual size fractions was less than but close to the measured value. These surface area values for individual size fractions and composite were within the range as previously determined for the <2 mm size fraction in Hanford 300A sediments.[5] Micropore volume, as calculated from the BJH method based on N_2 adsorption results (data not shown), decreased with increasing grain size with a much higher micropore volume in the clay/silt fraction (Table 2). The additively calculated micropore volume in the composite was close to the measured value.

U(VI) Adsorption Isotherms. U(VI) adsorption increased with decreasing grain size in equilibrium with aqueous U(VI) after normalizing to the solid mass in each size fraction (Figure 1A). There was a notable increase in U(VI) adsorption strength in the clay/silt fraction, consistent with its larger surface area and micropore volume (Table 2). All measured chemicals (pH, cations, and carbonate) in the suspensions had negligible changes before and after equilibration, thus excluding the influence of aqueous uranyl speciation changes on U(VI) adsorption in different size fractions. The slopes of all the isotherms gradually decreased with increasing aqueous U(VI) concentration, indicating that site saturation started to exert its effect on the isotherms despite the fact that only a small amount (<30 nmol/g) of U(VI) was adsorbed.

The isotherm for each size fraction was described using the same surface complexation reaction (eq 1) by adjusting two parameters: adsorption site concentration and equilibrium reaction constant. Preliminary model fits revealed that the fitted equilibrium reaction constants (log K, adjusted to zero ionic strength) for all size fractions had an average value of 24.72 with a standard deviation of 0.20. Consequently, in the final fit to each isotherm, the equilibrium constant was fixed (i.e., log K = 24.72), and only adsorption site concentration was adjusted. The effect of chemical composition on ionic activities in the SC reaction (eq 1) was considered through the aqueous speciation reactions. The SC model with the same surface complexation reaction and reaction constant well described the isotherms for all size fractions (Figure 1A) after considering size-specific sorption site concentration (Table 3). The estimated site concentration decreased with increasing grain size, consistent with a common concept that smaller size particles have a higher site concentration.[29] However, the estimated values of the site density after normalizing to surface area (5.10−1.72 nmol/m^2) were 3 orders of magnitude less than a generic surface site density of 3.84 μmol/m^2,[30] which has often been used in calculating uranyl surface complexation reactions in sediments.[5,9] A much lower adsorption site density was needed here to describe the decreasing slope of the isotherms with increasing aqueous concentration.

While the exact mechanism for this phenomenon was unclear, the result implied that there were two pools of uranyl adsorption sites in each grain-size fraction: strong and weak sorption sites. Only the strong site with a low sorption site density was revealed under our experimental condition. This was supported by the estimated log K value (24.72), which was 3 orders of magnitude higher than a log K value (21.64) estimated based on the generic site density in similar sediments collected from the Hanford IFRC site.[26] Other research has showed that two pools of adsorption sites were needed to describe uranyl adsorption on mineral surfaces and that adsorption was dominated by the strong site when uranyl loading was low.[16,31,32] The calculated K_d value for the various size fractions, which integrates the effect of site concentration and equilibrium constant, ranged from 2.4 to 12.7 mL/g when aqueous U(VI) was below 0.25 μmol/L (Table 3). The K_d value decreases with increasing aqueous U(VI) as indicated by the decreasing slope in adsorbed U(VI) as a function of aqueous U(VI) (Figure 1). These K_d values were consistent with those reported for other sediments from the 300A site when a generic site density was used.[26]

The estimated site concentration and calculated K_d values (Table 3) were generally correlated with size-specific surface area, but a better correlation was observed with micropore volume (Figure 2). Increasing micropore volume linearly increased th adsorption site concentration and K_d value, suggesting

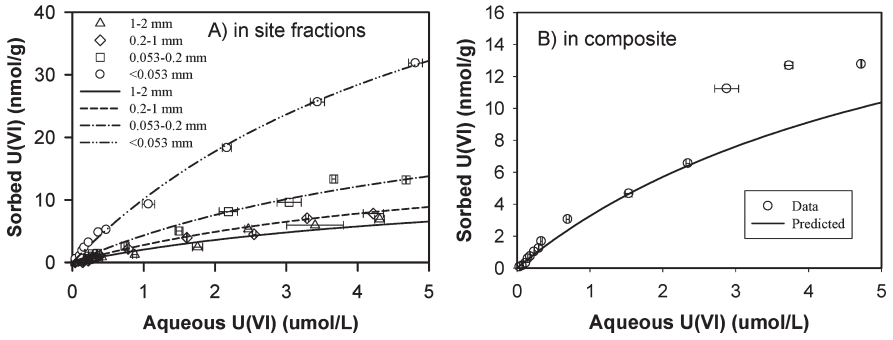

Figure 1. Measured (symbols) and calculated (lines) U(VI) adsorption isotherms in different size fractions (A) and their composite (B). Lines in plot A were fitted, and the solid line in plot B was calculated from the mass-weighted, linear addition of equilibrium U(VI) adsorption to four grain-size fractions, and the error bar denotes one standard deviation.

Table 3. Parameters Used in Modeling U(VI) Adsorption/Desorption

	size fraction (mm)			
	<0.053	0.053 < size < 0.2	0.2 < size < 1	1 < size < 2
site concentration (nmol/g)	69.0	29.5	19.0	14.0
equilibrium sorption constant (log K)	24.72	24.72	24.72	24.72
distribution coefficient (K_d, mL/g)	12.7	5.0	3.2	2.4
logarithm mean of rate constant, μ, ln(min^{-1})	−9.9	−9.9	−10.2	−10.8
deviation of log rate constant, σ, ln(min^{-1})	4.6	4.6	2.9	2.1
mean rate constant (min^{-1})[a]	1.9	1.9	2.5×10^{-3}	1.9×10^{-4}
median rate constant (min^{-1})[b]	5.0×10^{-5}	5.0×10^{-5}	3.7×10^{-5}	2.0×10^{-5}

[a] Mean rate constant = $\exp(\mu + \sigma^2/2)$. [b] Median rate constant = $\exp(\mu)$.

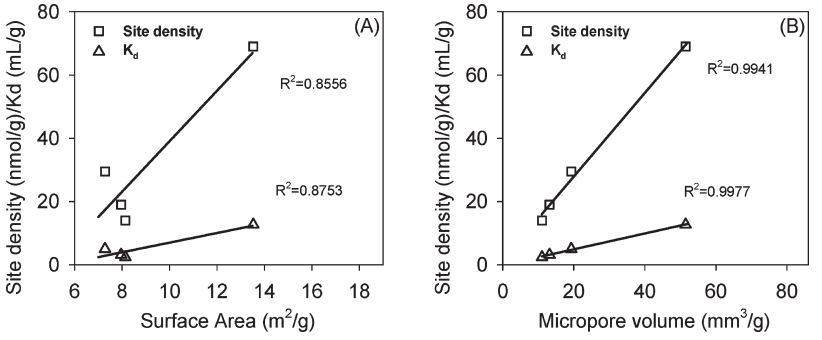

Figure 2. Correlation of the estimated site density and U distribution coefficient (K_d) with surface area (A) and micropore volume (B) in grain-size fractions.

that the micropore regions might be the preferred locations for uranyl adsorption. Microscopic observations of preferential uranium distribution inside grains and grain-coating domains in the Hanford sediments support this speculation.[21,27]

The calculated isotherms for individual grain-size fractions were used to evaluate the additivity concept of U(VI) adsorption. The isotherm from each size fraction was linearly added as a function of aqueous U(VI), weighted by their mass percentages in the composite. Numerically, the isotherm for the composite (Figure 1B) was calculated from the competitive surface complexation reactions in a mixture of four size mass fractions in a batch system. Here each size fraction had the same equilibrium constant (log K = 24.72) but with a size-specific sorption site concentration (Table 3) corrected by their mass percentages (Table 2) in the composite. The calculated composite isotherm was dominated by the contributions from larger size fractions, as indicated by the similarity between the calculated isotherm for the composite (Figure 1B) and the isotherms for the large size fraction, e.g., 0.2−1 mm (Figure 1A). This was because the large size fractions were present at much larger mass fractions. The calculated and measured isotherms matched well for the composite when the aqueous U(VI) concentration was below 2 μmol/L. Above 2.5 μmol/L, however, the calculated U(VI) adsorption was less than the measured value. The underprediction using the additive model was experimentally repeatable, suggesting that the smaller size fraction (clay/silt) with a stronger sorption affinity may have played a larger role than implied by its mass percentage. Coating of the large size fractions by silt/clay

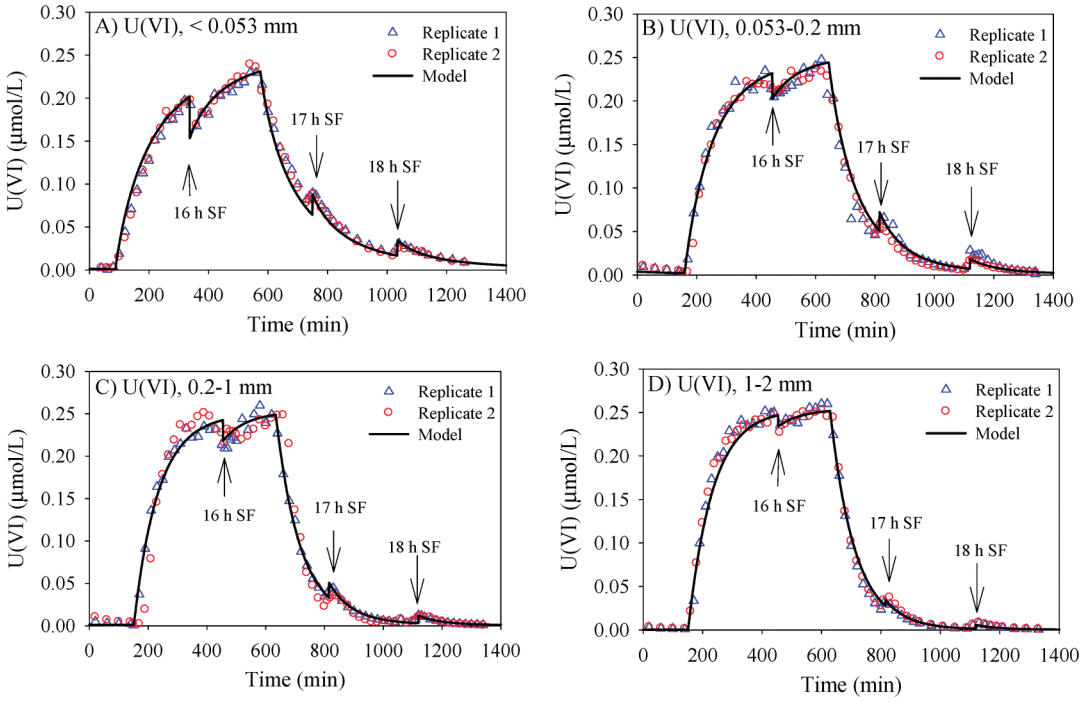

Figure 3. Measured (symbols) and calculated (lines) effluent concentrations of U(VI) in individual size fractions from a flow-cell reactor.

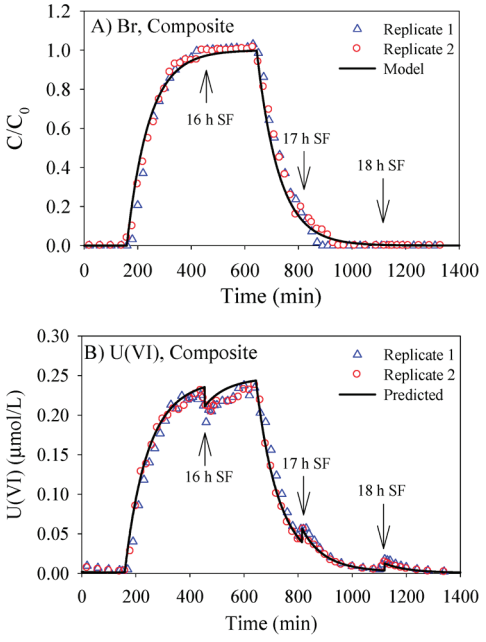

Figure 4. Measured (symbols) and calculated (lines) effluent concentrations of Br and U(VI) in the composite. The lines were calculated from the mass-weighted, linear addition of U(VI) adsorption/desorption kinetics in individual grain-size fractions.

materials in the composite may have created such a scenario. Nevertheless, contaminated groundwater often contains less than 2 μmol/L of aqueous U(VI).[27,33] Consequently, the linear additivity concept would be applicable under most field conditions.

U(VI) Adsorption and Desorption Kinetics. The kinetic U(VI) adsorption and desorption behavior was revealed for each size fraction and their composite by their response to the stop-flow (SF) events and through comparison to the tracer Br curves (Figures 3 and 4, Figure S1 in the Supporting Information). The 16 h SF event during the U(VI) injection phase caused a decrease in effluent U(VI) concentration when flow was restarted. This decrease was not observed for tracer Br and reflected the kinetic behavior of grain-scale U(VI) adsorption. The SF events during the U(VI) leaching phase (after 600 min) caused rebounding in effluent U(VI) concentration, which again was not observed for Br. The kinetic behavior of U(VI) adsorption/desorption was attributed to diffusion-limited surface complexation reactions within intragrain pore domains of the sediment. Br was also expected to have diffused into and out of intragrain regions during U(VI) adsorption/desorption. However, the ratio of micropore volume (Table 2) to bulk solution volume (11 mL) ranged from 0.3% to 1% in different grain-size fractions, indicating a relatively low storage capacity for the tracer Br in the intragrain domains. The negligible response of effluent Br to the SF events reflected this low storage capacity. The absence of intragrain retardation further diminished the effect of the SF events on Br effluent concentrations (Figure S1 in the Supporting Information). In contrast, a significant amount of U(VI) can be stored in the micropore domains through surface complexation reactions. The molar ratio of adsorbed U(VI) in intragrain pore domains to aqueous U(VI) in bulk solution ranged from 0.9 to 2.6 in different size fractions as calculated from U(VI) adsorption isotherms in Figure 1 and solid water ratio in the reactor. The high intragrain sorption capacity for U(VI) caused the retarded diffusion, which led to a measurable kinetic effect on U(VI) adsorption and desorption induced by the SF events.

The U(VI) effluent curves showed more skewed profiles in the smaller size fractions (Figure 3). Both sorption strength (site concentration in this case) and kinetic rate could affect the skewness in the breakthrough curves. A multirate surface complexation

model (eq 2 and 3) was used to separate the effect of these two factors by including size-specific site concentration in the kinetic model. Two parameters (μ and σ) for the rate constant distribution (eq 5) were estimated for each size fraction by matching calculated and measured effluent U(VI) concentrations. The multirate model (eq 2) well described the data in each size fraction (Figure 3) with fitted rate parameters provided in Table 3. The same set of the rate constants could describe adsorption and desorption for each size fraction. This is in contrast to the previous finding that the desorption was slower than the adsorption.[12] A likely reason is that the adsorption duration was short in this case and adsorbed U(VI) was reversible for desorption. The fitted rate constants indicated that the larger size fraction exhibited a slower reaction rate, as indicated by the mean or median rate constant for each site fraction calculated from μ and σ (Table 3). The larger skewness in the clay/silt fraction (Figure 3A), however, was mainly caused by the adsorption site concentration because the rate constant distribution in this size fraction was the same as those in the fine sand fraction (Table 3).

The multirate model with fitted parameters was used to test the additivity concept of U(VI) adsorption/desorption kinetics. Similarly to the adsorption isotherm case, U(VI) was allowed to competitively adsorb or desorb in the flow-cell reactor containing a mixture of four size fractions according to their mass percentage in the composite. The effluent U(VI) concentration was calculated using the combination of the multirate models developed for each size fraction scaled by their mass percentage. The calculated U(VI) effluents in the composite generally matched well with the measured values (Figure 4B). The Br in the composite (Figure 4A) was calculated by the same approach but with a zero reaction rate. The good match between calculated and measured effluents for both Br and U(VI) indicated that the additivity concept with respect to grain size was applicable. One cautious note for this conclusion is that the dominant minerals in our case were the same in all size fractions and solution chemical composition was the same in all experiments. Further research is needed to evaluate the additivity concept with respect to grain size under changing solution chemical composition and for sediments with variable mineral composition in different size fractions.

Implication. The SC model is a preferred approach to describe U(VI) adsorption and desorption in sediments because it allows explicit incorporation of the effects of chemical conditions on adsorption/desorption mass actions. A key factor in applying this approach is the surface complexation site concentration, which is often a sediment-specific property and changes with mineral surface areas.[30,34] A generic site density normalized to sediment surface area (3.84 μmol/m^2) has been proposed to calculate U(VI) adsorption site concentration in sediments.[30] In this approach, the surface site concentration for a specific sediment is calculated from the generic site density multiplied by the surface area, which is a parameter that is easier to measure. This study, however, found that sorption site concentration required to fit the adsorption isotherms was much lower than that calculated from the generic site density. The lower site concentration was likely caused by the preferential association of U(VI) with certain surface areas or sites such as those in the intragrain pores, whose concentration did not necessarily correlate with total surface area (Table 2). The observed linear additivity of uranyl adsorption with respect to grain size provided an alternative approach to estimate sorption site concentration based on grain-size distribution. In this proposed approach, the site concentration (S_t) for the composite (sediment) can be calculated using the following equation under condition that the same surface reaction and reaction constant can describe U(VI) adsorption/desorption in all size fractions

$$S_t = \sum_{i=1}^{N} w_i S_i \tag{6}$$

where S_i and w_i are the site concentration and mass percentage for size fraction i in the composite and N is the number of size fractions. Laboratory measurement/estimation of site concentration in representative size fractions is required for application of this approach. The field-measured grain-size distribution (w_i) can then be used to estimate the sorption site concentration from eq 6. The surface complexation reactions in the composite can be calculated using the additively calculated S_t without explicit calculations of surface complexation reactions in each size fraction. In cases when different surface complexation reactions have to be used to describe U(VI) adsorption in different size fractions, eq 6 is no longer applicable and the additive contribution to the composite from different size fractions will have to be competitively calculated and then added according to their mass percentage.

The kinetic behavior of U(VI) surface complexation may be described using a multirate SC model.[9] The rate constants in the multirate SC model, however, vary with sediment type and properties, even for those collected from the same field site.[12] The linear additivity property of U(VI) adsorption/desorption kinetics with respect to grain size as observed herein yields the following equation to calculate the rate constant of the composite (sediment)

$$\alpha_j^k(\text{composite}) = \frac{\sum_{i=1}^{N} w_i \alpha_j^k(\text{size } i)(Q_j^k(\text{size } i) - q_j^k(\text{size } i))}{\sum_{i=1}^{N} w_i (Q_j^k(\text{size } i) - q_j^k(\text{size } i))} \tag{7}$$

where α_j^k(composite) and α_j^k(size i) are the rate constant of adsorbed species j at sorption site k in the composite and in the size fraction i, respectively, and Q_j^k(size i) and q_j^k(size i) are the equilibrium and currently adsorbed U(VI) concentration in size fraction i. Equation 7 indicates that the rate constants in the composite are a function of the rate constants and adsorbed concentrations in each size fraction. Consequently, the kinetic behavior in each size fraction has to be explicitly calculated to simulate the kinetic behavior of the composite.

■ ASSOCIATED CONTENT

Supporting Information. Effluent tracer Br concentrations in the stirred flow-cell experiments that correspond to the results in Figure 3. This material is available free of charge via the Internet at http://pubs.acs.org.

■ AUTHOR INFORMATION

Corresponding Author

*Phone: (509)371-6350; fax: (509)371-6354; e-mail: Chongxuan.Liu@pnl.gov.

■ ACKNOWLEDGMENT

This research was funded by the U.S. Department of Energy (DOE) Office of Biological and Environmental Research (BER) Division through a Subsurface Biogeochemical Research Program (SBR) Science Focus Area (SFA) program at Pacific Northwest National Laboratory (PNNL). Part of the research and experiments was performed at the Environmental Molecular Science Laboratory (EMSL), a DOE national user facility located at PNNL. PNNL is operated by Battelle Memorial Institute under subcontract DE-AC06-76RLO 1830. We thank four anonymous reviewers and Associate Editor Dr. Dzombak for valuable comments and suggestions.

■ REFERENCES

(1) Sparks, D. L. *Environmental Soil Chemistry*; Academic Press, Inc.: San Diego; 1995.

(2) Davis, J. A.; Meece, D. E.; Kohler, M.; Curtis, G. P. Approaches to surface complexation modeling of uranium(VI) adsorption on aquifer sediments. *Geochim. Cosmochim. Acta* **2004**, *68*, 3621–3641.

(3) Liu C. X.; Zachara J. M.; Qafoku N. P.; Wang Z. Scale-dependent desorption of uranium from contaminated subsurface sediments. *Water Resour. Res.* **2008**, *44*, W08413; doi 08410.01029/02007WR006478.

(4) Um, W.; Icenhower, J. P.; Serne, C. F.; Wang, Z. M.; Dodge, C. J.; Francis, A. J. Characterization of uranium-contaminated sediments from beneath a nuclear waste storage tank from Hanford, Washington: Implications for contaminant transport and fate. *Geochim. Cosmochim. Acta* **2010**, *74*, 1363–1380.

(5) Bond, D. L.; Davis, J. A.; Zachara, J. M. Uranium (VI) release from contaminated vadose zone sediments: Estimation of potential contributions from dissolution and desorption. In *Adsorption of Metals by Geomedia II: Variable Mechanisms, and Model Applications*; Barnett, M. O., Kent, D. B., Eds.; Elsevier: Amsterdam, Netherlands, 2008; pp 375−416.

(6) Curtis, G. P.; Fox, P.; Kohler, M.; Davis, J. A. Comparison of in-situ uranium Kd Values with a laboratory determined surface complexation model. *Appl. Geochim.* **2004**, *19*, 1643–1656.

(7) Gajowiak, A.; Majdan, M.; Drozdzal, K. Sorption of uranium(VI) on clays and clay minerals. *Przem. Chem.* **2009**, *88*, 190–196.

(8) Kohler, M.; Curtis, D. P.; Meece, D. E.; Davis, J. A. Methods for estimating adsorbed uranium(VI) and distribution coefficients of contaminated sediments. *Environ. Sci. Technol.* **2004**, *38*, 240–247.

(9) Liu, C. X.; Shi, Z.; Zachara, J. M. Kinetics of uranium(VI) desorption from contaminated sediments: effect of geochemical conditions and model evaluation. *Environ. Sci. Technol.* **2009**, *43*, 6560–6566.

(10) Palagyi, S.; Laciok, A. Sorption, desorption and extraction of uranium from some sands under dynamic conditions. *Czech. J. Phys.* **2006**, *56*, D483–D492.

(11) Payne, T. E.; Edis, R.; Fenton, B. R.; Waite, T. D. Comparison of laboratory uranium sorption data with 'in situ distribution coefficient' at the Koongarra uranium deposit, Northern Australia. *J. Environ. Radioact.* **2001**, *57*, 35–55.

(12) Qafoku, N. P.; Zachara, J. M.; Liu, C.; Gassman, P. L.; Qafoku, O.; Smith, S. C. Kinetic desorption and sorption of U(VI) during reactive transport in a contaminated Hanford sediment. *Environ. Sci. Technol.* **2005**, *39*, 3157–3165.

(13) Curtis G. P.; Davis J. A.; Naftz D. L. Simulation of reactive transport of uranium(VI) in groundwater with variable chemical conditions. *Water Resour. Res.* **2006**, *42*, W04404; doi:04410.01029/02005WR003979.

(14) Zhu, C.; Hu, F. Q.; Burden, D. S. Multi-component reactive transport modeling of natural attenuation of an acid groundwater plume at a uranium mill tailing site. *J Contam. Hydrol.* **2001**, *52*, 85–108.

(15) Yabusaki S. B.; Fang Y.; Waichler S. R. Building conceptual models of field-scale uranium reactive transport in a dynamic vadose zone-aquifer-river system. *Water Resour. Res.* **2008**, *44*, W12403; doi:12410.11029/12007WR006617.

(16) Barnett, M. O.; Jardine, P. M.; Brooks, S. C. U(VI) adsorption to heterogeneous subsurface media: application of a surface complexation model. *Environ. Sci. Technol.* **2002**, *36*, 937–942.

(17) Davis, J. A.; Coston, J. A.; Kent, D. B.; Fuller, C. C. Application of the surface complexationconcept to complex minerals assemblages. *Environ. Sci. Technol.* **1998**, *32*, 2820–2828.

(18) Honeyman B. D. Cation and anion adsorption at the oxide/solution interface in systems containing binary mixtures of adsorbents: An inverstigation of the concept for adsorptive additivity. Ph.D. Thesis, Stanford Univesity, Stanford, CA, 1984.

(19) Waite, T. D.; Davis, J. A.; Fenton, B. R.; Payne, T. E. Approaches to modeling uranium(VI) adsorption on natural mineral assemblages. *Radiochim. Acta* **2000**, *88*, 687–693.

(20) Miller, A. W.; Rodriguez, D. R.; Honeyman, B. D. Upscaling sorption/desorption processes in reactive transport models to describe metal/radionuclide transport: A critical review. *Environ. Sci. Technol.* **2010**, *44*, 7996–8007.

(21) Stubbs, J. E.; Veblen, L. A.; Elbert, D.; Zachara, J. M.; Davis, J. A.; Veblen, D. R. Newly recognized hosts for uranium in the Hanford Site vadose zone. *Geochim. Cosmochim. Acta* **2009**, *73*, 1563–1576.

(22) Ewing R. P.; Hu Q.; Liu C. Scale dependence of intragranular porosity, tortuosity, and diffusivity. *Water Resour. Res.* **2010**, *46*, W06513; doi:06510.01029/02009WR008183.

(23) Barrett, E. P.; Joyner, L. G.; Halenda, P. P. The determination of pore volume and area distributions in porous substance. I. Computations from nitrogen isotherms. *J. Am. Chem. Soc.* **1951**, *73*, 373–380.

(24) Joyner, L. G.; Barrett, E. P.; Skold, R. The determination of pore volume and area distribution in porous substances. 2. Comparison between nitrogen isotherm and mercury porosimeter methods. *J. Am. Chem. Soc.* **1951**, *73*, 3155–3158.

(25) Gregg, S. J.; Sing, K. S. W. *Adsorption, Surface Area, and Porosity*; Academic Press, Inc.: New York, 1982.

(26) Stoliker, D. L.; Kent, D. B.; Zachara, J. M. Application of surface complexation modeling to evaluate differences in equilibrium uranium-(VI) adsorption properties of aquifer sediments. *Environ. Sci. Technol.* **2011**submitted for publication.

(27) Zachara, J. M.; Davis, J. A.; Liu, C.; McKinley, J. P.; Qafoku, N. P.; Wellman, D. M.; Yabusaki, S. B. Uranium Geochemistry in Vadoze Zone and Aquifer Sediments from the 300 Area Uranium Plume, PNNL-15121; Pacific Northwest National Laboratory: Richland, WA, 2005.

(28) Tokunaga, T. K.; Olson, K. R.; Wan, J. M. Moisture characteristics of Hanford gravels: Bulk, grain-surface, and intragranular components. *Vadose Zone J* **2003**, *2*, 322–329.

(29) Zeng, H.; Singh, A.; Basak, S.; Ulrich, K.-U.; Sahu, M.; Biswas, P.; Catalano, J. G.; Giammar, D. E. Nanoscale size effects on uranium-(VI) adsorption to hematite. *Environ. Sci. Technol.* **2009**, *43*, 1373–1378.

(30) Davis, J. A.; Kent, D. B. Surface complexation modeling in aqueous geochemistry. In: *Mineral-Water Interface Geochemistry, Reviews in Mineralogy*. Edited by Hochella, M. F., White, A. F. Mineralogical Society of America: Washington, DC, 1990; pp 177−260.

(31) Waite, T. D.; Davis, J. A.; Payne, T. E.; Waychunas, G. A.; Xu, N. Uranium(VI) adsorption to ferrihydrite: Application of a surface complexation model. *Geochim. Cosmochim. Acta* **1994**, *58*, 5465–5478.

(32) Davis, J. A. Surface complexation modeling of uranium(VI) adsorption on natural mineral assemblages. US Geological Survey: Menlo Park, CA, 2001; p 214, NUREG/CR-6708.

(33) Fang, Y.; Yabusaki, S. B.; Morrison, S. J.; Amonette, J. P.; Long, P. E. Multicomponent reactive transport modeling of uranium bioremediation field experiments. *Geochim. Cosmochim. Acta* **2009**, *73*, 6029–6051.

(34) Dzombak, D. A.; Morel, F. M. M. *Surface Complexation Modeling*; Wiley-Interscience: New York, 1990.